Progress In Electromagnetics Research M, Vol. 32, 169–180, 2013

DESIGN OF OPTICAL DEVICES BASED ON HYBRID PERIODIC/FIBONACCI PHOTONIC CRYSTAL IN THE VISIBLE AND THE NEAR INFRARED DOMAINS

Abir Mouldi* **and Mounir Kanzari**

Laboratoire de Photovoltaique et Matériaux Semi Conducteurs, Ecole Nationale d'Ingénieurs de Tunis, BP 37, Le Belvédère, Tunis 1002, Tunisie

Abstract—In this work, we exploit photonic crystal heterostructures formed by the combination of periodic and Fibonacci structures to design promising optical devices acting in the visible and the near infrared domains. An hybrid structure of the type Bragg mirror-$(\text{Fibonacci})^{S}$ is proposed to enhance the high reflection band through the one dimensional photonic crystal in the near infrared. The use of the configuration exhibits a large photonic band gap at any angle of incidence and for both polarizations. The proposed structure is a quarter wavelength omnidirectional mirror of 37 layers with a bandwidth larger than that of the periodic structure with an increasing ratio 3.7, and it covers all the optical telecommunication wavelengths 0.85, 1.3 and 1.55 µm. Then a second structure of the type Bragg mirror-$(\text{Fibonacci})^{S}$-Bragg mirror with varied optical thicknesses permits to confine strongly the light giving a rise to a microcavity through the visible range with strong mode localisation. Since different physical phenomena have their own relevant physical scales, we exploit the physical properties of the proposed structures in different wavelength domains to obtain different optical devices. The transmission spectra are determined by using a theoretical model based on the Transfer Matrix Method (TMM).

Received 17 June 2013, Accepted 10 August 2013, Scheduled 19 August 2013
* Corresponding author: Abir Mouldi (abir20052002@yahoo.fr).

1. INTRODUCTION

Photonic Crystals (PCs) or Photonic Band Gap (PBG) materials are a new class of optical nanostructures with a periodic modulation in the dielectric constants on the length scale comparable to optical wavelength. These artificial materials create a range of forbidden frequencies in which propagation of electromagnetic wave is completely prohibited. Their capability of microscopically manipulating the flow of photons leads to the design and development of futuristic photonic devices with improved performances [1–5]. We cite as examples of PC devices, resonant microcavities and omnidirectional mirrors which are precisely the subject of the present work. A microcavity is an optical resonator close to, or below the dimension of the wavelength of light. The most common cavities are created by the insertion of local imperfections that trap light at a point within the crystal [6], but some works are interested by creating microcavities by the using of heterostructures [7]. Photonic crystal heterostructures are formed by joining two or more photonic crystals into a single structure, which gives the heterostructure a more complex band structure than that of a periodic photonic crystal [8]. Photonic crystal heterostructures have been successfully used to develop devices such as high-quality resonant cavities [7] and mirrors with large omnidirectional Photonic Band Gap (PBG) [9, 10]. The heterostructure revealed in this paper is the combination of periodic and quasi periodic photonic crystals which is the Fibonacci photonic crystal.

2. METHOD OF CALCULATION

For the calculation of system reflection and transmission, we employed the Transfer Matrix Method (TMM). It is based on Abeles method [11–14] in terms of forward and backward propagating electric field, that is, E^+ and E^- which were introduced to calculate the reflection and transmission. Abeles showed that the relation between the amplitudes of the electric fields of the incident wave E_0^+, reflected wave E_0^-, and transmitted wave after m layers, E_{m+1}^+, is expressed as the following matrix for stratified films within m layers:

$$\begin{pmatrix} E_0^+ \\ E_0^- \end{pmatrix} = \frac{C_1 C_2 C_3 \dots C_{m+1}}{t_1 t_2 t_3 \dots t_{m+1}} \begin{pmatrix} E_{m+1}^+ \\ E_{m+1}^- \end{pmatrix} \tag{1}$$

Here, C_j is the propagation matrix with the matrix elements.

$$C_j = \begin{pmatrix} \exp(i\phi_{j-1}) & r_j \exp(-i\phi_{j-1}) \\ r_j \exp(i\phi_{j-1}) & \exp(-i\phi_{j-1}) \end{pmatrix} \tag{2}$$

where t_j and r_j are the Fresnel transmission and reflection coefficients, respectively, between the $(j-1)$th and jth layer. The Fresnel coefficients t_j and r_j can be expressed as follows by using the complex refractive index $\hat{n}_j = n_j + ik_j$ and the complex refractive angle θ_j. For Transverse Magnetic (TM) polarization (Parallel polarization):

$$r_{jTM} = \frac{\hat{n}_{j-1}\cos\theta_j - \hat{n}_j\cos\theta_{j-1}}{\hat{n}_{j-1}\cos\theta_j + \hat{n}_j\cos\theta_{j-1}} \tag{3}$$

$$t_{jTM} = \frac{2\hat{n}_{j-1}\cos\theta_{j-1}}{\hat{n}_{j-1}\cos\theta_j + \hat{n}_j\cos\theta_{j-1}} \tag{4}$$

Moreover, for Transverse Electric (TE) polarization (Perpendicular polarization):

$$r_{jTE} = \frac{\hat{n}_{j-1}\cos\theta_{j-1} - \hat{n}_j\cos\theta_j}{\hat{n}_{j-1}\cos\theta_{j-1} + \hat{n}_j\cos\theta_j} \tag{5}$$

$$t_{jTE} = 2\frac{\hat{n}_{j-1}\cos\theta_{j-1}}{\hat{n}_{j-1}\cos\theta_{j-1} + \hat{n}_j\cos\theta_j} \tag{6}$$

The complex refractive indices and the complex angles of incidence obviously follow Snell's law: $\hat{n}_{j-1}\sin\theta_{j-1} = \hat{n}_j\sin\theta_j$ $(j = 1, 2, \ldots, m+1)$. The values ϕ_{j-1} in Equation (2) indicate the change in the phase of the wave between $(j-1)$th and jth boundaries and are expressed by the equation:

$$\phi_0 = 0 \tag{7}$$

$$\phi_{j-1} = \frac{2\pi}{\lambda}\hat{n}_{j-1}d_{j-1}\cos\theta_{j-1} \tag{8}$$

Except for $j = 1$, λ is the wavelength of the incident light in vacuum and d_{j-1} the thickness of the $(j-1)$th layer. By putting $E^-_{m+1} = 1$, because there is no reflection from the final phase, Abeles obtained a convenient formula for the total reflection and transmission coefficients, which correspond to the amplitude reflectance r and transmittance t, respectively, as follows:

$$r = \frac{E^-_0}{E^+_0} = \frac{c}{a} \tag{9}$$

$$t = \frac{E^+_{m+1}}{E^+_0} = \frac{t_1 t_2 \ldots t_{m+1}}{a} \tag{10}$$

The quantities a and c are the matrix elements of the all product C_j matrix:

$$C_1 C_2 C_3 \ldots C_{m+1} = \begin{pmatrix} a & b \\ c & d \end{pmatrix} \tag{11}$$

By using Equations (9) and (10), we can easily obtain the energy reflectance R as:

$$R = |r|^2 \tag{12}$$

For (TM) and (TE) polarizations and the energy transmittance T as:

$$T_{TE} = \mathrm{Re}\left(\frac{\hat{n}_{m+1}\cos\theta_{m+1}}{\hat{n}_0\cos\theta_0}\right)|t_{TE}|^2 \tag{13}$$

$$T_{TM} = \mathrm{Re}\left(\frac{\cos\theta_{m+1}/\hat{n}_{m+1}}{\cos\theta_0/\hat{n}_0}\right)\left|\frac{\hat{n}_{m+1}}{\hat{n}_0}t_{TE}\right|^2$$

$$= \mathrm{Re}\left(\frac{\hat{n}_{m+1}\cos\theta_{m+1}}{\hat{n}_0\cos\theta_0}\right)|t_{TM}|^2 \tag{14}$$

for TE and TM polarization, respectively, where Re indicates the real part.

3. MODEL

The first system under consideration is a multiple of a generalized Fibonacci multilayer $[F_l(m,n)]^S$ combined with a periodic multilayer structure $(LH)^p$, S is the repetition number of the Fibonacci stack, p is the period's number of the Bragg multilayer. The Fibonacci block is composed of two layers H and L stacked alternatively along z direction and following the rules of Fibonacci sequence, that is $S_{l+1} = S_l^m S_{l-1}^n$ for $l \geq 1$ with $S_0 = L$ and $S_1 = H$, l is the generation number, m and n are parameters characterizing substitution rules generating the sequence. In fact, each transition from a generation to the following one is obtained by doing the substitutions $\rightarrow L^m H^n$, $H \rightarrow L$ or by using the relation between S_{l+1}, S_l and S_{l-1} [13].

To explain what change in generation number implies, we give the layers sequences of the different generations when $m = 2$ and $n = 3$

$S_0 = H$
$S_1 = L$
$S_2 = S_1^2 S_0^3 = LLHHH$
$S_3 = S_2^2 S_1^3 = LLHHHLLHHHLLL$
$S_4 = S_3^2 S_2^3$
$= LLHHHLLHHHLLLLLHHHLLHHHLLLLLHHHLLHHHLLHHH$
.....

Here, H and L are defined as two dielectric materials with H the high refractive index material and L the low refractive index material. Refractive indices of these materials are assumed to be constant in

the wavelength region of interest. We assume the individual layers as quarter-wave layers so satisfying the Bragg condition $n_H d_H = n_L d_L = \frac{\lambda_0}{4}$ with λ_0 is the reference wavelength. The second system considered in the visible range is a multiple of a generalized Fibonacci multilayer $[F_l(m,n)]^S$ embedded between two periodic multilayer structures $(LH)^p$, that is, the structure is built according to the form $(LH)^p[F_l(m,n)]^S(LH)^p$. Figure 1 shows an example of the considered structure.

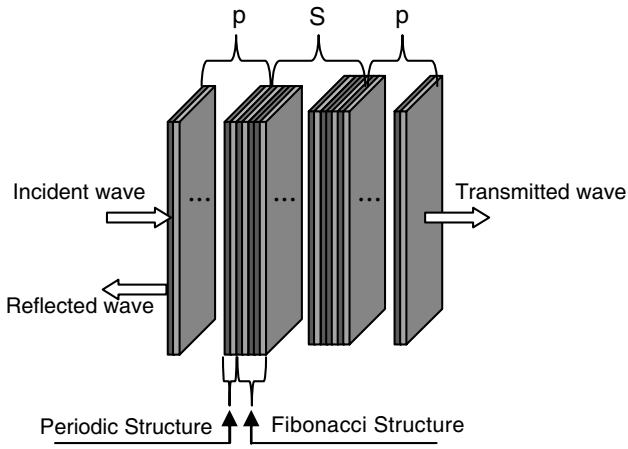

Figure 1. Schematic representation showing the geometry of the structure $(LH)^j[F_1(m,n)]^p(LH)^j$ with $m = n = 1$, $l = 3$.

4. RESULTS AND DISCUSSION

4.1. Enhancement of the Omnidirectional PBG in the Infra Red Range

In the infra red range, we utilize the Si as the high refractive index layer and SiO2 the as the low one. Si is a good candidate for the fabrication of photonic devices in the near-infrared and it is compatible with Si-based Microelectronics. So, the high and low refractive indices are taken to be $n_H = 3.7$ and $n_L = 1.45$. The reference wavelength is chosen here to be $\lambda_0 = 1.1\,\mu$m. This implies that the geometric thicknesses of layers are $d_H = 0.0743\,\mu$m and $d_L = 0.1896\,\mu$m. The proposed structure has the form $(LH)^p[F_l(m,n)]^S$, the parameters m, n, l, S and p are chosen to have the biggest PBG without peaks emerging through the band. The optimized structure is $(LH)^8[F_3(1,1)]^7$. So it is a multilayer of 37 quarter wave layers,

in a practical view point, the structure is simple to fabricate. In order to evaluate its response under different angles, we represent the omnidirectional band achieved with the conventional periodic structure $H(LH)^p$ with $p = 18$, so the total number of layers is 37 layers. Figure 2(a) shows the transmission spectra of the system with a quarter wave stacks as a function of the wavelength under normal incidence. Figure 2(b) gives the calculated variations of the photonic band gap edges as function of the incident angle varying between 0° and 90° for the *TE* polarization and the *TM* polarization (band diagram). We can see that the *TM* polarization bandwidth is broader than at normal incidence, whereas the *TE* polarization bandwidth is narrower. From this figure we can see that as the incident angle increases, the center wavelengths of both reflection bands shift to the shorter-wavelength region. We also note that the omnidirectional PBGs for the *TM* polarization are completely located within that for the *TE* polarization. Thus, the omnidirectional PBG for any polarization is the omnidirectional PBG for the *TM* polarization. Therefore, the omnidirectional PBG for both *TE* and *TM* polarizations can be defined by the edges of the upper photonic band at the incident angle of 90° and the lower photonic band at the normal incidence. Dark region represents the omnidirectional band. For this typical system, the width of the omnidirectional PBG is 0.2 μm.

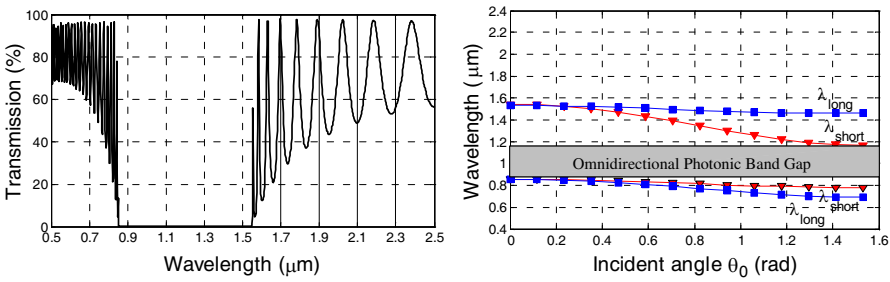

Figure 2. Transmission response of the periodic multilayer. (a) Transmssion spectrum under normal incidence. (b) Band edges shift as function of incident angle. Red curves represent transmission bands under *TM* polarization; Blue curves represent transmission bands under *TE* polarization.

Now, if we investigate the response of the hybrid structure $(LH)^8[F_3(1,1)]^7$, we obtain the results showed in Figure 3. It is clear from the figure that the band gap is extended to cover a very large spectrum and it exists for the two modes of polarization under all

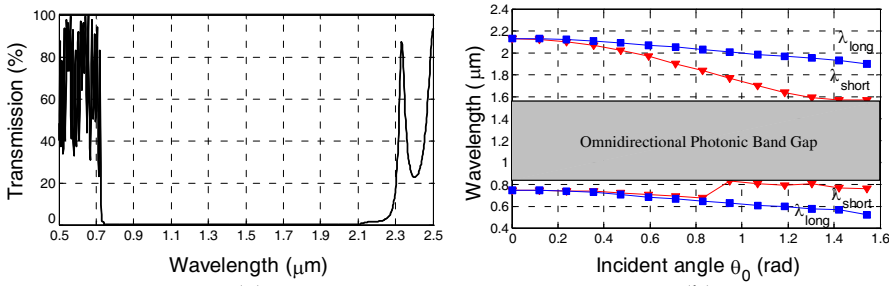

Figure 3. Transmission response of the hybrid multilayer $(LH)^8[F_3(1,1)]^7$. (a) Transmission spectrum under normal incidence. (b) Band edges shift as function of incident angle. Red curves represent transmission bands under *TM* polarization; Blue curves represent transmission bands under *TE* polarization.

incident angles from 0° to 90°.

Figure 3(b) shows the band diagram of the studied structure. Here we define the range of omnidirectional PBG for both *TE* and *TM* polarization is from the smallest value of the upper band edge to the largest value of the lower band edge under *TM* polarization. The range of the obtained omnidirectional forbidden band is from 0.825 μm to 1.563 μm. So the width of the omnidirectional band is 0.738 μm. therefore, with the same number of quarter wave layers as the periodic stack but with a different arrangement of high and low refractive indices layers, we achieve a large omnidirectional PBG with an increasing ratio comparing with the periodic structure of 3.7. We must also mention that the new extended omnidirectional PBG covers all the optical telecommunication wavelengths which are 0.85, 1.3, and 1.55 μm. Another work [14] led to the broadening of the omnidirectional reflection band covering these optical telecommunication wavelengths using a deformed Fibonacci PC. This was achieved with the 15th generation of the deformed Fibonacci structure so with 610 layers. Thus, the realizing of this band is limited by the practical limitation to stacking many layers and to control layers thicknesses with a deformation law. To explain how the proposed structure permitted to have the obtained results, we are reminded that the photonic band gap of a photonic crystal can be enlarged by using heterostructures [9]. The constituent 1D photonic crystals have to be properly chosen such that photonic band gaps of the adjacent photonic crystals overlap each other [9].

If we plot the transmission spectra of the periodic stack PC1

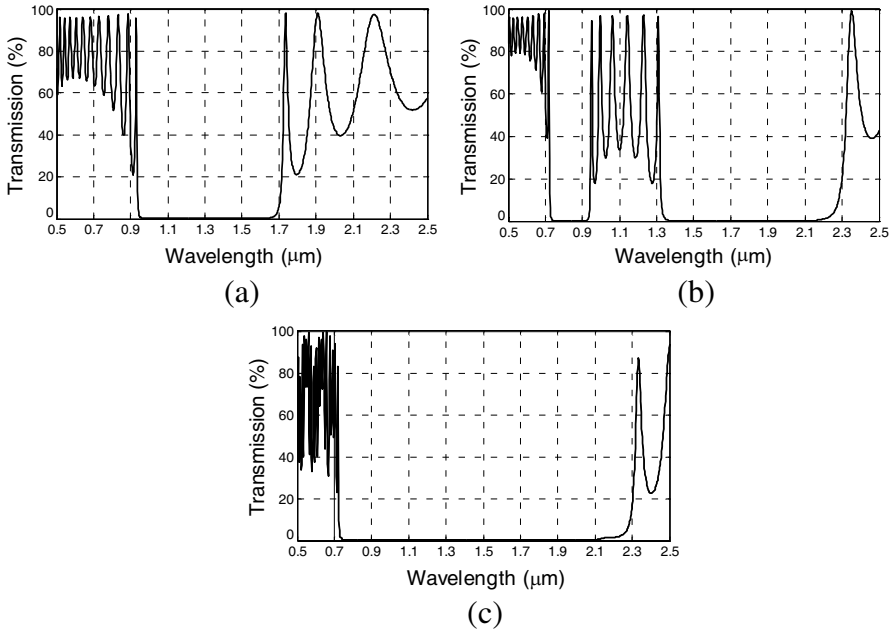

Figure 4. Transmission response under normal incidence of (a) the periodic multilayer $(LH)^8$, (b) the concatenated Fibonacci structure $[F_3(1,1)]^7$, (c) the hybrid structure $(LH)^8[F_3(1,1)]^7$.

having the form $(LH)^8$ (Figure 4(a)) and that of the quasiperiodic stack PC2 with the arrangement $[F_3(1,1)]^7$ (Figure 4(b)), we understand that the extended photonic band gap obtained through the structure PC3 with the form $(LH)^8[F_3(1,1)]^7$ (Figure 4(c)) is the result of the overlap of the PC1 band with the two bands obtained in the transmission spectrum of PC2. It is worth noting that the two bands of the PC2 are on the both sides of the PC1 band. This means that the band of PC1 compensates the central part between the two bands of the PC2 while the two bands of the PC2 compensate the two sides of the PC1 band. Finally, a very broad reflection band can be obtained by the combination of the two structures. From Figure 5 which represents the transmission spectra of PC1, PC2 and PC3 under grazing angles for the *TM* polarization, we see that each of the three considered bands exhibit an omnidirectional reflection and they overlap each other at different angles. So, it is the simultaneous adjacency of the PBGs under *TM* polarization at all incident angles which leads to the formation of the extended omnidirectional PBG. Connecting a second periodic stack at the upper edge of the structure

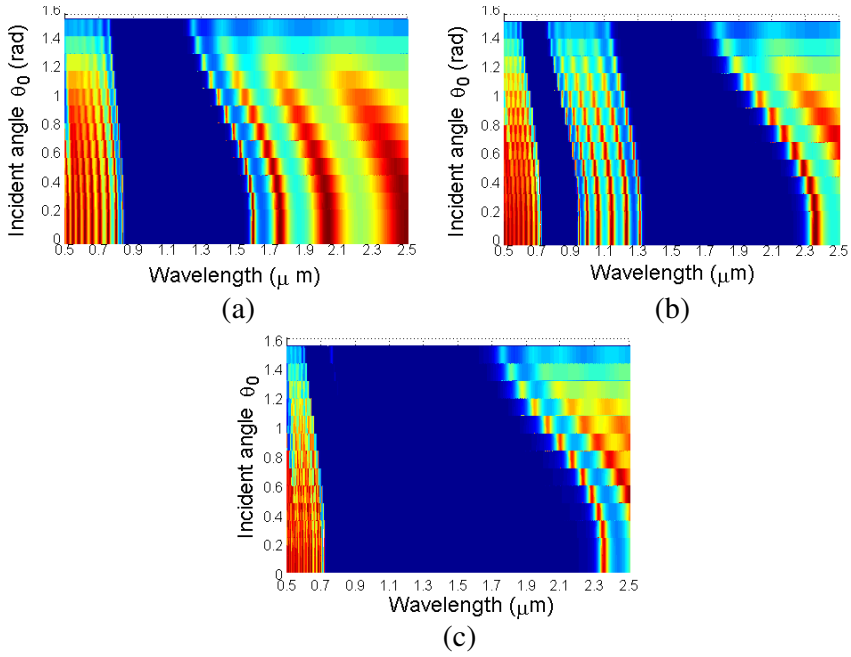

Figure 5. Transmission response under grazing angle of (a) the periodic multilayer $(LH)^8$, (b) the concatenated Fibonacci structure $[F_3(1,1)]^7$, (c) the hybrid structure $(LH)^8[F_3(1,1)]^7$.

permits to more extend the omnidirectional photonic band gap. The optimized structure with this configuration is $(LH)^8[F_3(1,1)]^7(LH)^8$, so the number of layers is 53. In this case, the omnidirectional PBG is extended from 0.821 μm to 1.679 μm so the width is 0.858 μm. But since our aim is the optimization of the structure response with a minimized number of layers, we consider the structure $(LH)^8[F_3(1,1)]^7$ with 37 layers the better to design a large omnidirectional photonic band gap in the infra red range.

4.2. Photonic Crystal Heterostructure Microcavity in the Visible Range

In the visible range, the high and low refractive indices are taken to be $n_H = 2.34$ and $n_L = 1.45$ which are the reflection indices of respectively the TiO2 and the SiO2. The micro cavity was designed by stacking quarter wavelength layers in according to the configuration $(LH)^p[F_l(m,n)]^S(LH)^p$. It is obtained by optimizing the structure parameters such as the generation number l, the Fibonacci

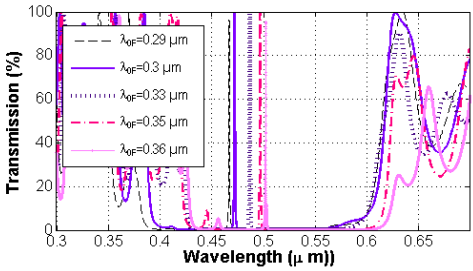

Figure 6. Transmission spectra of the hybrid structure $(LH)^8[F_3(1,1)]^8(LH)^8$ in the visible range, the reference wavelength of the Fibonacci sequences λ_{0F} is different from 0.5 μm.

parameters m and n, the repetition number S, the period's number p and the reference wavelengths λ_0 of each block. With the structure $(LH)^8[F_3(1,1)]^8(LH)^8$ in which the reference wavelength in the two sidewall periodic stacks is chosen to be $\lambda_0 = 0.5\,\mu$m, and that of the Fibonacci stacks is $\lambda_0 = 0.35\,\mu$m, we achieved a transmission peak at $\lambda_0 = 0.5\,\mu$m of more than 99.5% of transmission and with high quality factor, defined as $\Delta\lambda/\lambda$, of $Q = 1000$. So, in this case, the Fibonacci part $[F_3(1,1)^8]$ of the structure is acting as a "defect" which sharply defined microcavity with strong mode localization. Figure 6 shows that the peak can be modulated by varying the reference wavelength of the Fibonacci blocks between 0.3 and 0.35 μm, outside of this interval, the microcavity becomes a weak transmission peak (Transmission of the peak is under 97%).

Using the configuration with varying the reference wavelength of the Fibonacci stacks does not exhibit the same resonant transmission mode in the infra red range. This would be explained when we are reminded that layers are very thick (in the periodic stack, $d_H = 0.0534\,\mu$m and $d_L = 0.0862\,\mu$m) when the structure is acting in the visible range, so the response of the system is very sensitive to layer thicknesses variation so to the reference wavelength variation.

5. CONCLUSION

In this paper, engineered combinations of periodic and Fibonacci quasiperiodic structures are proposed. A broad omnidirectional PBG that results from special mutual compensation is obtained in the near infrared range to cover all the optical telecommunication wavelengths 0.85, 1.3 and 1.55 μm. The central idea is that the stop bands of the adjacent PCs exhibit omnidirectional reflection and overlap each other.

The advantage of this work over previous studies is the necessity for only 37 layers to have an omnidirectional PBG which is 3.7 times larger than that of the periodic structure, and also the structure is very simple since it has quarter wavelength layers. In the visible range, we exploit the approach of hybrid structure by sandwiching several Fibonacci multilayers between two sidewall Bragg mirrors and using different optical thicknesses into the structure. The idea is to use the Fibonacci block as a defect which leads to the emerging of a resonant microcavity. The resonant wavelength can be modulated by controlling the reference wavelength of the Fibonacci block so the optical thicknesses of its layers. Unlike the previous devices, the proposed structures are simple to fabricate and show very interesting optical properties.

REFERENCES

1. Mouldi, A. and M. Kanzari, "Broad multilayer antireflection coating by apodized and chirped photonic crystal," *Opt. Com.*, Vol. 284, 4124–4128, 2011.
2. Mouldi, A., M. Kanzari, and B. Rezig, "Broad antireflection grating by apodization of one dimensional photonic crystal," *PIERS Proceedings*, 1461–1464, Marrakesh, Morocco, Mar. 20–23, 2011.
3. Mouldi, A. and M. Kanzari, "Influence of the optical parameters on transmission properties of the chirped photonic crystal," *ACES Journal*, Vol. 26, No. 3, 259–266, 2011.
4. Mouldi, A. and M. Kanzari, "Design of an omnidirectional mirror using one dimensional photonic crystal with graded geometric layers thicknesses," *Optik*, Vol. 123, No. 2, 125–131, 2012.
5. Mouldi, A. and M. Kanzari, "Effects of punctual defects on the optical properties of the one-dimensional photonic crystals," *Phys. Chem. News*, Vol. 50, 14–22, 2009.
6. Tomljenovic-Hanic, S., C. M. de Sterke, M. J. Steel, B. J. Eggleton, Y. Tanaka, and S. Noda, "High-Q cavities in multilayer photonic crystal slabs," *Opt. Express.*, Vol. 15, No. 25, 17248–17253, 2007.
7. Escorcia-Garcia, J. and M. E. Mora-Ramos, "Study of optical propagation in hybrid periodic/quasiregular structures based on porous silicon," *PIERS Online*, Vol. 5, No. 2, 167–170, 2009.
8. Cox, J. D., J. Sabarinatha, and M. R. Singh, "Resonant photonic states in coupled heterostructure photonic crystal waveguides," *Nanoscale Res. Let.*, 741–746, 2010.

9. Han, P. and H. Wang, "Criterion of omnidirectional reflection in a one-dimensional photonic heterostructure," *J. Opt. Soc. Am. B*, Vol. 22, No. 7, 1571–1575, 2005.
10. Srivastava, R., S. Pati and S. P. Ojha, "Enhancement of omnidirectional reflection in photonic crystal heterostructure," *Progress In Electromagnetics Research B*, Vol. 1, 197–208, 2008.
11. Li, Z.-Y., "Principles of the plane-wave transfer-matrix method for photonic crystals," *Science and Technology of Advanced Materials*, Vol. 6, No. 7, 837–841, Oct. 2005.
12. Zeng, Y., Y. Fu, X. Chen, W. Lu, and H. Ågren, "Extended plane-wave-based transfer-matrix approach to simulating dispersive photonic crystals," *Solid State Communications*, Vol. 139, No. 7, 328–333, Aug. 2006.
13. Mouldi, A. and M. Kanzari, "Design of microwave devices exploiting Fibonacci and hybrid periodic/Fibonacci one dimensional photonic crystals," *Progress In Electromagnetics Research B*, Vol. 40, 221–240, 2012.
14. Ben Abdelaziz, K., J. Zaghdoudi, M. Kanzari, and B. Rezig, "A broad omnidirectional reflection band obtained from deformed Fibonacci quasi-periodic one dimensional photonic crystals," *J. Opt. A: Pure Appl. Opt.*, Vol. 7, 544–549, 2005.